MASSIVE YOUNG CLUSTERS IN THE DISK OF M31

F. Fusi Pecci, M. Bellazzini, A. Buzzoni, E. De Simone, and L. Federici

INAF–Osservatorio Astronomico di Bologna, Via Ranzani 1, 40127 Bologna, Italy; flavio.fusipecci@bo.astro.it,
michele.bellazzini@bo.astro.it, alberto.buzzoni@bo.astro.it, luciana.federici@bo.astro.it

AND

S. Galleti[1]

Dipartimento di Astronomia, Universitá di Bologna, Via Ranzani 1, 40127 Bologna, Italy; silvia.galleti2@unibo.it

ABSTRACT

We have studied the properties of a sample of 67 very blue and likely young massive clusters in M31 extracted from the Bologna Revised Catalog of globular clusters, selected according to their color [$(B - V)_0 \leq 0.45$] and/or the strength of their Hβ spectral index (H$\beta \geq 3.5$ Å). Their existence in M31 has been noted by several authors in the past; we show here that these blue luminous compact clusters (BLCCs) are a significant fraction ($\gtrsim 15\%$) of the whole globular cluster system of M31. Compared to the global properties of the M31 globular cluster system, they appear to be intrinsically fainter and morphologically less concentrated, with a shallower Balmer jump and enhanced Hβ absorption in their spectra. Empirical comparison with integrated properties of clusters with known ages, as well as with theoretical simple stellar population models, consistently indicates that their typical age is less than ~ 2 Gyr, so they are probably not as metal-poor as would be deduced if they were older. When selecting BLCCs by either their $(B - V)_0$ colors or the strength of their Hβ index, the cluster sample turns out to be distributed on the outskirts of the M31 disk, sharing the kinematic properties of the thin, rapidly rotating disk component. If confirmed to be young and not metal-poor, these clusters indicate the occurrence of significant recent star formation in the thin disk of M31, although they do not set constraints on the epoch of its early formation.

Key words: galaxies: evolution — galaxies: individual (M31) — globular clusters: general — Local Group

1. INTRODUCTION

Globular clusters (GCs) are ubiquitous stellar systems living in any kind of galaxy, from dwarfs to giants and from the earliest to the latest types. Their integrated properties carry crucial information about the physical characteristics of their host galaxy at the time of its formation. Hence, the study of GC systems is a fundamental tool for understanding the evolutionary history of the baryonic component of distant galaxies (see Harris 2001 and references therein).

In this framework, the GC system of the Andromeda galaxy (M31) plays a twofold role: as a natural reference to compare with the Milky Way (MW) GC population and as a fundamental test bed for the techniques to be applied to systems in more distant galaxies (see Barmby et al. 2000; Puzia et al. 2002; Rich 2003; Barmby 2003; Galleti et al. 2004; and references therein). Indeed, the comparison of the GC system of M31 and the MW has revealed both fundamental similarities and interesting differences, whose complete understanding may have a deep impact on our knowledge of galaxy formation and evolution (Hodge 1992; van den Bergh 2000; Morrison et al. 2004; Beasley et al. 2004; Burstein et al. 2004).

Among the differences, in the present contribution we especially focus on the claimed presence in M31 of stellar systems similar to MW GCs in luminosity and shape but with integrated colors significantly bluer than the bluest MW counterparts. While some of the faintest objects can hardly be distinguished from bright open clusters (OCs), the typical family member appears quite similar to classical GCs (two typical examples are shown in Fig. 1;[2] see Williams & Hodge 2001a, 2001b; Hodge 1979). In § 3.4 we provide some evidence suggesting that clusters of similar age and total luminosity may be lacking in the MW. Hereafter, we call them "blue luminous compact clusters" (BLCCs).[3]

The peculiar colors of BLCCs were first reported by Vetešnik (1962), van den Bergh (1967, 1969), and Searle (1978), and this class of objects then received growing attention (Crampton et al. 1985; Cowley & Burstein 1988; Elson & Walterbos 1988; King & Lupton 1991; Bohlin et al. 1993; Barmby et al. 2000; Williams & Hodge 2001a; Beasley et al. 2004; Burstein et al. 2004), although a systematic study is still lacking.

In particular, Elson & Walterbos (1988) noted 14 such blue clusters not included in the list of OC candidates by Hodge (1979) and more consistent with a GC morphology. Their absolute luminosities spanned the luminosity range $-9.5 < M_V < -6.5$, and their positions in a two-color diagram pointed to a possibly young age. For 10 of these objects, King & Lupton (1991) provided supplementary $UBVR$ photometry indicating a global luminosity around 3×10^4–4×10^5 $L_\odot$. Based on stellar population models, their estimated age appeared to be less than a few times 10^8 yr, with a typical mass between 3×10^3 and 5×10^4 $M_\odot$. If confirmed, these values indicate that they are higher than those of Galactic OCs but comparable to those of the young, rich GCs found in the Large Magellanic Cloud (Elson & Fall 1985; van den Bergh 1991).

---

[1] Also at INAF–Osservatorio Astronomico di Bologna, Via Ranzani 1, 40127 Bologna, Italy.

[2] Frames for Fig. 1 have been retrieved from the WFPC2 associations archive at http://archive.stsci.edu/hst/wfpc2/index.html.

[3] We do not attach any special meaning to this newly introduced term. It is intended only as a convenient label describing the color and structural morphology of these clusters to be used in the following for the sake of brevity and clarity.
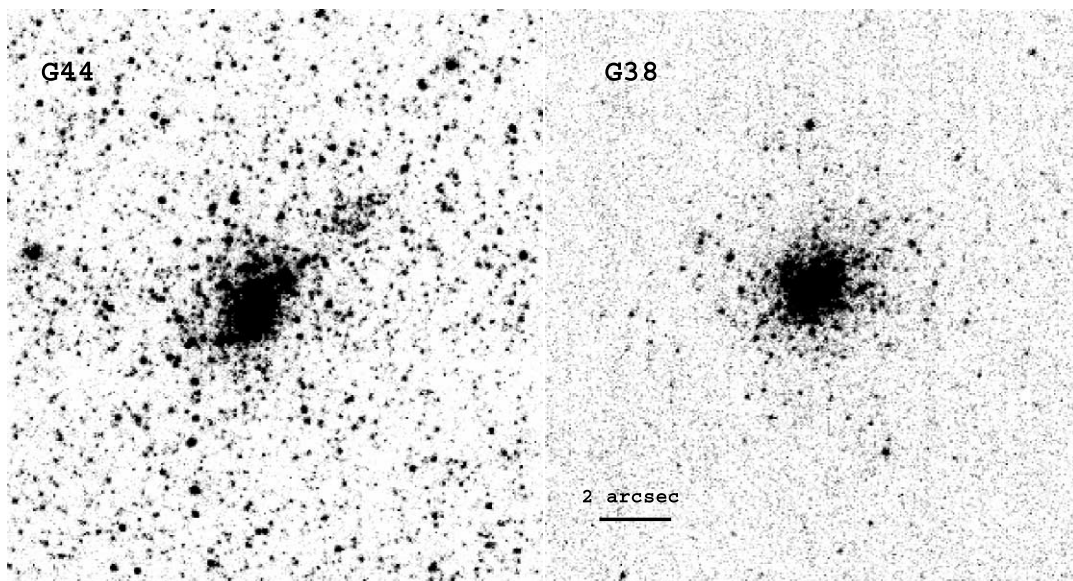
Fig. 1.—BLCCs G38 and G44 from the *HST* WFPC2 observations by Williams & Hodge (2001a).

Bohlin et al. (1988, 1993), studying the UV colors of a sample of 49 GC candidates in M31, listed 11 objects classified as blue clusters based on their location in the two-color diagram and suggested that they are probably young. In the same line of investigation, Barmby et al. (2000) noted that their M31 catalog of GC candidates could be contaminated by several young objects with $B - V < 0.55$, and they eventually excluded 55 such objects from their analysis of old M31 clusters.

As already stressed long ago (Spinrad & Schweizer 1972), the integrated spectrum and color of a cluster, especially in the blue, are influenced by the metal abundance and the position of the main-sequence turnoff (MSTO) stars (and in turn, by the cluster age), by the strength of the horizontal branch (HB), and, to a lesser degree, by the overall luminosity function (LF) of its stellar population. To disentangle the different effects, it is thus very important to obtain the color-magnitude distribution of cluster stellar populations. In this regard, Williams & Hodge (2001a) obtained deep *Hubble Space Telescope* (*HST*) photometry of individual stars and color-magnitude diagrams for four of these BLCCs, leading to estimated ages in the range of 60–160 Myr and metallicity from solar to 2/5 solar. This clearly supports the evidence that the exceedingly blue integrated colors of BLCCs are a direct consequence of their remarkably young ages.

Beasley et al. (2004) reached similar conclusions for eight BLCCs by comparing high-quality, low-resolution spectra of a sample of M31 clusters with similar data for MW and Magellanic Cloud GCs. Burstein et al. (2004) reported a global sample of 19 BLCCs in M31, including 13 "young" objects from the Barmby et al. (2000) survey,[4] most of them sharing the kinematic properties of a wider sample of "red" clusters belonging to the cold thin disk detected by Morrison et al. (2004).

In summary, various observations suggest that M31 may have many more young GCs than the MW, and the latest results on the claimed existence of a thin disk subsystem of GCs in M31, quite large in number and covering a very wide range in metallicity from $[Fe/H] < -2.3$ up to solar and above (Perrett et al. 2002; Morrison et al. 2004), have opened an important debate and actually gave rise to the present study.

In fact, as recently discussed by Morrison et al. (2004), Beasley et al. (2004), and Burstein et al. (2004), and references therein, the detection of several old metal-poor clusters with thin disk kinematics would imply that (1) M31 is likely to have had a disk already in place at the very early stages of the galaxy evolution, and (2) no substantial merger event can have occurred at later epochs, as the galaxy disk would have been disrupted or, at least, heated (but see, however, Abadi et al. 2003). This conclusion is at odds with the indications found by Brown et al. (2003), who reported the detection of a wide intermediate-age (6–8 Gyr) population of metal-rich stars (with $[Fe/H] > -0.5$) in a minor-axis halo field of M31 observed with the *HST* ACS, interpreted as the result of the merging with an almost equal-mass companion. As a consequence, it is of primary interest to verify if and how many clusters do belong to the claimed thin disk and, even more important, how old and metal-poor they are.

In § 2 we carry out a revision and a new selection of the candidate sample of BLCCs based on different (and partially complementary) criteria, relying on the Bologna Revised Catalog (BRC) of M31 GCs (Galleti et al. 2004).[5] Then, in § 3 we discuss the properties of the global sample of clusters and in particular their kinematic properties, metallicity, and estimated ages.

We anticipate that our analysis will lead us to conclude that most (if not all) of the BLCCs are younger than ~ 2 Gyr and more metal-rich than $[Fe/H] \sim -1.0$ and that they nicely fit the structural and kinematic characteristics of the thin disk subsystem recently detected by Morrison et al. (2004). This issue is further discussed in § 4, in which we also summarize the main results of our analysis.

2. TOWARD A FAIR SAMPLING OF BLCCs IN M31

To carry out a systematic analysis of the BLCC population of the Andromeda galaxy, our BRC data have been complemented with the kinematic and spectral indices information from Perrett et al. (2002). This choice allowed us to preserve full homogeneity in the comparison of line indices and to take advantage at the same time of a larger sample of clusters and a better accuracy of radial velocity measurements. It has to be noted,

---

[4] Barmby et al. (2000) classified these clusters as possibly young because of the strong Balmer absorption lines observed in their high-resolution spectra.

[5] See the latest electronic version of the catalog available at the Web address http://www.bo.astro.it/M31.

TABLE 1
ADOPTED BLCC SAMPLES

Name	V	$B-V$	$U-B$	$\langle[Fe/H]\rangle$	Δ (mag)	Hβ (Å)	$W_{1/4}$	V_r (km s^{-1})	δ	X (arcmin)	Y (arcmin)	Sample	References
B008-G060..............	16.56	1.10	0.50	-0.41 ± 0.38	0.397	3.50	4.96	-319	0.70	-15.34	19.95	B	
B028-G088..............	16.86	0.88	-0.05	-1.87 ± 0.29	0.404	3.81	4.80	-434	0.72	-23.65	2.67	B	1
B040-G102..............	17.38	0.29	-0.01	-0.98 ± 0.48	0.137	7.41	5.32	-463	-0.40	-35.48	-11.77	A, B	2, 3, 4, 5
B043-G106..............	16.96	0.28	-0.14	-2.42 ± 0.51	0.144	5.53	5.13	-414	0.42	-33.68	-11.21	A, B	2, 3, 4, 5, 6, 7, 8, 9
B047-G111	17.51	0.72	0.09	-1.62 ± 0.41	. . .	3.53	5.57	-291	-1.02	13.80	24.58	B	
B049-G112..............	17.56	0.52	0.18	-2.14 ± 0.55	. . .	9.31	5.83	-481	-0.39	-27.56	-7.27	A, B	5
B057-G118..............	17.64	0.69	. . .	-2.12 ± 0.32	0.289	5.56	4.98	-437	0.27	-25.00	-7.02	B	
B066-G128..............	17.42	0.36	-0.27	-2.10 ± 0.35	0.061	4.67	4.95	-389	0.70	-29.61	-13.02	A, B	4, 5, 6, 8
B069-G132..............	18.16	0.44	0.02	-1.35 ± 0.43	0.338	7.17	5.72	-295	-0.27	3.44	11.91	A, B	1, 5
B074-G135..............	16.65	0.75	0.14	-1.88 ± 0.06	0.346	3.92	5.15	-435	-5.61	17.38	22.06	B	
B081-G142..............	16.80	0.54	0.26	-1.74 ± 0.40	0.352	7.98	4.99	-430	-0.47	-25.32	-12.23	A, B	5
B083-G146..............	17.09	0.76	0.06	-1.18 ± 0.44	0.047	3.75	5.75	-367	-4.15	19.90	22.04	B	
B091-G151..............	17.56	0.41	0.02	-1.80 ± 0.61	0.269	7.30	5.02	-290	-0.16	2.08	7.01	A, B	1, 5, 7
B114-G175..............	17.28	0.42	0.33	. . .	. . .	. . .	4.90	. . .	. . .	-3.87	-0.58	A	1
B160-G214..............	18.02	0.55	0.05	-1.17 ± 1.25	. . .	. . .	4.78	-354	-0.46	-7.98	-13.45	A	1
B170-G221..............	17.39	0.98	0.53	-0.54 ± 0.24	. . .	4.52	4.63	-295	1.54	-15.59	-21.43	B	
B210-M11	17.57	0.52	0.02	-1.90 ± 0.32	0.162	6.83	4.98	-265	0.11	7.69	-12.70	A, B	1, 5, 10
B216-G267..............	17.25	0.20	0.02	-1.87 ± 0.39	0.177	5.66	5.72	-84	-0.10	26.91	0.92	A, B	1, 3, 5, 6, 8, 9, 10
B222-G277..............	17.43	0.68	0.47	-0.93 ± 0.95	0.349	8.47	6.91	-311	-1.07	10.14	-16.17	B	1, 11
B223-G278..............	17.81	0.15	0.14	-1.13 ± 0.51	0.297	4.44	5.65	-101	-0.01	26.39	-3.81	A, B	1, 5, 10
B237-G299..............	17.10	0.77	0.16	-2.09 ± 0.28	0.167	7.43	5.08	-86	4.54	21.81	-17.48	B	
B281-G288..............	17.67	0.84	0.50	-0.87 ± 0.52	0.364	5.56	6.20	-203	0.76	16.85	-15.09	B	
B295-G014..............	16.75	0.71	0.27	-1.71 ± 0.15	. . .	4.77	4.92	-423	. . .	-85.95	19.69	B	9
B303-G026..............	18.22	0.24	0.46	-2.09 ± 0.41	0.252	5.78	5.46	-464	1.84	-65.51	5.53	A, B	5
B307-G030..............	17.32	0.87	1.01	-0.41 ± 0.36	. . .	5.76	6.35	-407	3.02	-57.96	4.58	B	
B314-G037..............	17.63	0.59	0.34	-1.61 ± 0.32	0.402	5.19	6.48	-485	0.51	-69.94	-10.77	B	6, 9, 11
B315-G038..............	16.47	0.07	0.02	-2.35 ± 0.54	0.116	4.77	5.18	-559	-0.18	-55.65	-0.83	A, B	2, 3, 5, 6, 8, 9, 10, 12
B318-G042..............	17.02	0.17	-0.42	. . .	. . .	. . .	5.31	. . .	. . .	-52.16	-1.09	A	2, 3, 5, 6, 7, 8, 9
B319-G044..............	17.61	0.72	-0.64	-2.27 ± 0.47	0.113	5.37	5.49	-535	0.21	-52.03	-1.54	B	2, 3, 5, 6, 8, 12
B321-G046..............	17.67	0.22	0.22	-2.39 ± 0.41	0.229	6.29	5.52	-518	-0.05	-55.54	-7.17	A, B	5, 6, 9, 10, 11
B322-G049..............	17.75	0.06	-0.28	. . .	. . .	. . .	5.14	. . .	. . .	-46.31	-0.57	A	4, 5, 9, 10, 11
B327-G053..............	16.58	0.32	-0.35	-2.33 ± 0.49	0.160	4.09	4.87	-528	0.25	-47.70	-3.23	A, B	4, 5, 6, 7, 8, 9, 10, 11
B331-G057..............	18.19	0.25	. . .	. . .	. . .	. . .	6.31	. . .	. . .	4.76	36.35	A	
B342-G094..............	17.73	0.30	0.64	-1.62 ± 0.02	0.003	7.06	6.52	-479	-0.66	-40.46	-12.04	A, B	2, 3, 4, 5, 12
B354-G186..............	17.81	0.13	0.69	. . .	. . .	. . .	5.45	. . .	. . .	35.36	26.68	A	
B355-G193..............	17.76	0.53	0.02	-1.62 ± 0.43	0.240	4.39	4.24	-114	5.25	34.00	24.37	A, B	

TABLE 1—*Continued*

Name	V	$B - V$	$U - B$	$\langle$[Fe/H]$\rangle$	Δ (mag)	Hβ (Å)	$W_{1/4}$	V_r (km s^{-1})	δ	X (arcmin)	Y (arcmin)	Sample	References
B358-G219..............	15.22	0.49	0.19	...	...	...	5.06	...	...	−64.79	−58.32	A	
B367-G292..............	18.45	0.32	−0.17	−2.32 ± 0.53	0.097	6.21	5.64	−152	−0.58	53.03	12.32	A, B	5
B368-G293..............	17.92	0.26	−0.36	...	...	...	5.75	...	...	41.80	3.36	A	2, 3, 5, 6, 8, 12
B374-G306..............	18.31	0.44	0.33	−1.90 ± 0.67	0.281	4.07	5.27	−96	0.88	41.08	−10.68	A, B	5
B376-G309..............	18.06	0.45	0.23	...	...	...	5.59	...	...	42.12	−10.79	A	5, 6, 8, 9
B380-G313..............	17.01	0.47	0.33	−2.31 ± 0.45	0.187	6.52	6.67	−13	1.14	58.47	−2.07	A, B	5, 9, 10, 11
B431-G027..............	17.73	0.49	0.29	...	...	...	5.59	...	...	−59.11	9.36	A	5
B443-D034..............	18.20	0.80	−0.52	−2.37 ± 0.46	...	6.72	5.40	−532	−0.08	−50.47	−4.58	B	
B448-D035..............	17.49	0.61	0.01	−2.16 ± 0.19	...	6.70	6.54	−552	−0.16	−43.17	−2.77	B	5
B451-D037..............	18.66	0.19	...	−2.13 ± 0.43	...	3.50	4.40	−514	0.20	−33.01	2.57	A, B	5
B453-D042..............	17.30	0.87	0.16	−2.09 ± 0.53	0.234	4.12	5.27	−446	0.47	−23.69	5.79	B	
B458-D049..............	17.84	0.49	0.91	−1.18 ± 0.67	−0.085	6.19	5.98	−521	−0.83	−26.50	−6.22	A, B	5
B475-V128..............	17.56	0.31	0.10	−2.00 ± 0.14	...	5.96	7.24	−120	−1.02	45.00	3.92	A, B	5
B480-V127..............	17.91	0.65	0.39	−1.86 ± 0.66	0.188	5.19	4.89	−135	−0.50	44.30	−8.38	B	
B483-D085..............	18.46	0.27	0.08	−2.96 ± 0.35	...	5.58	5.87	−53	−0.09	58.16	0.58	A, B	5
B484-G310..............	18.10	0.52	0.58	−1.95 ± 0.59	0.110	5.70	5.45	−104	0.06	46.62	−8.51	A, B	5, 10
B486-G316..............	17.52	0.35	0.93	...	...	...	5.02	...	...	9.45	−41.39	A	5
B189D-G047............	...	...	...	−1.19 ± 0.29	−0.064	4.24	...	−584	−0.62	−45.82	0.24	B	
VDB 0...................	15.28	0.23	−0.37	...	...	...	...	...	...	−47.41	−4.31	A	4, 6, 7, 8
NB 21−AU 5	17.86	0.31	...	...	...	...	...	...	...	−0.88	0.85	A	
NB 67−AU 13	16.14	0.48	−0.03	−1.43 ± 0.13	...	...	...	−113	1.66	1.69	3.75	A	5
NB 83....................	16.68	0.56	−0.03	−1.26 ± 0.16	...	...	...	−150	1.30	−4.24	0.89	A	
B006D-D036............	18.00	...	...	−2.16 ± 0.32	−0.026	5.04	...	−522	0.51	−36.31	2.25	B	
B012D-D039............	18.40	...	...	−1.22 ± 0.41	0.182	7.09	...	−478	−0.10	−26.72	6.07	B	
B015D-D041............	17.80	...	...	−1.14 ± 0.30	...	7.32	...	−445	−0.41	−19.24	9.37	B	
B111D-D065	18.10	...	...	−1.80 ± 0.36	0.082	5.55	...	−130	−0.81	27.38	2.27	B	
B195D....................	15.19	0.22	−0.30	−1.64 ± 0.19	0.166	4.29	...	−552	−0.45	−47.19	−4.17	A, B	
B206D-D048............	19.06	0.12	...	−2.01 ± 0.99	...	2.53	...	−490	−0.07	−27.97	−6.40	A	
B257D-D073............	17.40	...	...	−1.99 ± 0.19	0.501	5.49	...	−114	−1.25	46.00	3.87	B	
DAO 47..................	...	...	...	−1.13 ± 0.57	0.229	4.03	...	−490	−0.35	−33.09	−7.67	B	
V031......................	17.43	0.68	0.39	−1.59 ± 0.06	0.497	5.84	...	−433	0.02	−19.01	7.27	B	10

REFERENCES.—(1) Jiang et al. 2003; (2) van den Bergh 1967; (3) Sargent et al. 1977; (4) Bohlin et al. 1993; (5) Barmby et al. 2000; (6) Elson & Walterbos 1988; (7) Bohlin et al. 1988; (8) King & Lupton 1991; (9) Barmby & Huchra 2001; (10) Burstein et al. 2004; (11) Beasley et al. 2004; (12) Williams & Hodge 2001a.
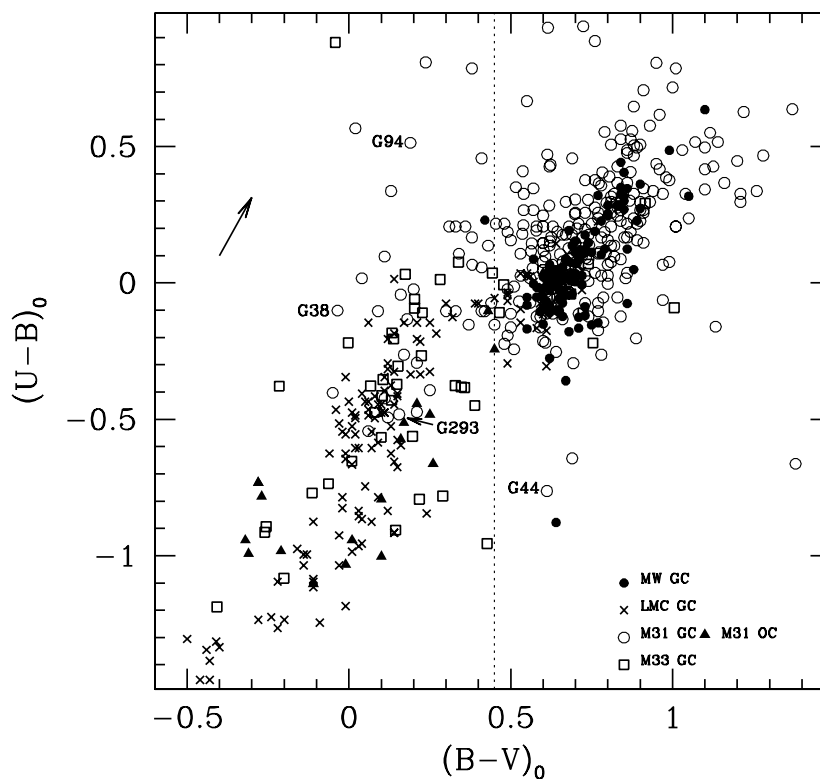
Fig. 2.—Two-color diagram of GCs for Local Group galaxies. Data for M31 GCs are from the BRC (Galleti et al. 2004; *open circles*), those for the MW are from Harris (1996; *filled circles*), LMC GCs are from van den Bergh (1981; *crosses*), and M33 data are from Chandar et al. (1999; *squares*). Also reported in the plot are the M31 OCs from the Hodge (1979) catalog (*triangles*). All the data have been reddening-corrected assuming $E(B - V) = 0.11$ for M31, 0.13 for LMC, and 0.07 for M33. MW GCs have been corrected according to Harris (1996). Note the broader color distribution of M31 GCs compared to the MW population. The vertical line marks the reference value $(B - V)_0 = 0.45$ adopted for the BLCC selection. Labeled clusters are those observed by Williams & Hodge (2001a) with *HST*. The arrow is a reddening vector for $E(B - V) = 0.1$ mag.

however, that our main conclusions remain essentially unchanged if the Brodie & Huchra (1990) data set is used instead.

Throughout this paper, for M31 we assume a distance modulus $(m - M)_0 = 24.43$ mag (Freedman & Madore 1990), a systemic radial velocity $V_r = -301$ km s^{-1}, and an *X-Y* coordinate system referred to the galaxy center (both from van den Bergh 2000). A single value for the interstellar extinction toward the galaxy is adopted for simplicity, with $E(B - V) = 0.11$ (McClure & Racine 1969; Hodge 1992) and a standard reddening law (e.g., Scheffler 1982). As discussed in more detail below (§ 2.1), this simple assumption has little effect on the essence of the results presented. For example, we verified that our results would remain substantially unaffected when using, alternatively, the individual reddening values provided by Barmby et al. (2000).

All the M31 clusters comprised in our analysis (i.e., the 67 targets collected in Table 1) belong to class 1 BRC entries; that is, they are all *genuine* M31 members confirmed either spectroscopically or by means of high-resolution imaging.[6] The clusters are selected according to their intrinsic color [i.e., $(B - V)_0 \leq 0.45$] and/or the strength of their Hβ spectral index (H$\beta \geq 3.5$ Å). The rationale of these selection criteria is explained in detail in the following sections.

2.1. *Color Selection*

Figure 2 is a collection of the GC population for Local Group galaxies in the reddening-corrected $U - B$ versus $B - V$ color

plane. We joined data for the MW (Harris 1996 and the latest updates),[7] the LMC (van den Bergh 1981), M33 (Chandar et al. 1999), and M31 (Galleti et al. 2004). For the MW GCs, the adopted values of the color excess $E(B - V)$ are those originally provided by Harris (1996), while $E(B - V) = 0.13$ for the LMC and 0.07 for M33 (van den Bergh 2000).

As a well-recognized feature, the large majority of M31 GCs in the figure tend to bunch around $(B - V)_0 \simeq 0.7$ and closely track the locus of the MW GCs, suggesting a similar age and metallicity distribution. On the other hand, as noted long ago by Vetešnik (1962), van den Bergh (1967, 1969), and more recently by Barmby et al. (2000), several M31 GCs are spread over much bluer colors, compatible with the young and intermediate-age LMC GCs.[8]

On the basis of the $B - V$ distribution of Figure 2, a more immediate selection criterion for BLCCs in M31 is to pick up those objects bluer than the bluest GC in the MW [i.e., NGC 7492,[9] with $(B - V)_0 \sim 0.42$; Harris 1996]. Operationally, we therefore defined a color-selected BLCC sample (referred to as sample A in our following discussion) consisting of 41 objects (out of 330 confirmed GCs in M31, according to BRC) with $(B - V)_0 \leq 0.45$. These objects are reported in Table 1 (with

---

[6] Two original class 1 BRC objects, namely, B430-G025 and NB 91, eventually were found to be foreground field stars from a deeper analysis (Galleti et al. 2004; Beasley et al. 2004) and have been excluded from the present sample.

[8] Note, however, that some of the most extreme M31 outliers in the Fig. 2 plot are probably due to poor photometry in one (likely U) of the *UBV* bands and/or to inaccurate reddening correction. See Barmby et al. (2000) and Galleti et al. (2004) for a detailed discussion of M31 GC photometry.

[9] This is a quite conservative choice, since NGC 7492 appears to be exceptionally blue. All other Galactic GCs in the Harris catalog have $(B - V)_0 \geq 0.57$.
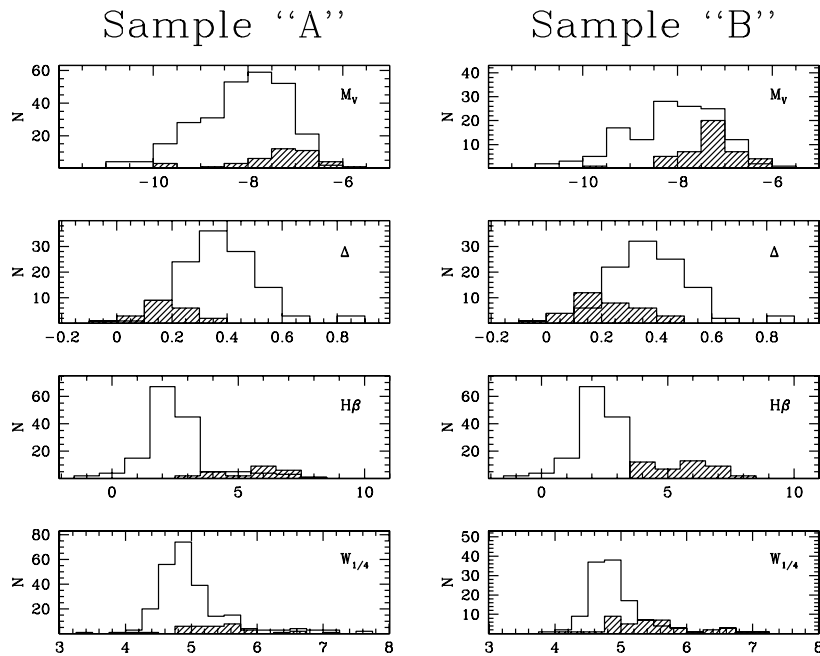
Fig. 3.—*Left panels*: Distribution of color-selected BLCCs (sample A; *hatched histograms*) and ordinary clusters with $(B - V)_0 > 0.45$ (*open histograms*) vs. absolute V magnitude (*top*), the 4000 Å Balmer-break index Δ (in magnitude scale, according to Brodie & Hanes [1986]; *second from top*), the Lick Hβ pseudo–equivalent width (in Å, according to Faber et al. [1985]; *second from bottom*), and the $W_{1/4}$ morphological parameter (according to Buonanno et al. [1982]; Battistini et al. [1987]; *bottom*). *Right panels*: Same as the left panels but for the Hβ-selected BLCCs (sample B; *hatched histograms*) vs. ordinary clusters, now defined as those with H$\beta < 3.5$ (*open histograms*).

the label "A" in the second to last column); of these, 29 targets have radial velocity estimates in the list of Perrett et al. (2002). We are aware, of course, that the indicative threshold in the integrated $B - V$ color might be too "prudent" a selection, as, for instance, it misses cluster G44 (see Fig. 2), claimed by Williams & Hodge (2001a) to have an age of about 100 Myr on the basis of the *HST* color-magnitude diagram. On the other hand, the other three young clusters of Williams & Hodge (2001a) are correctly picked up, and in any case the relevant uncertainty in the reddening correction for most of the M31 clusters prevents any firm selection criterion based on integrated colors alone. Therefore, sample A likely provides a clean conservative estimate of the real fraction of young objects in the M31 GC population, and certainly secures our statistics from any contamination of intrinsically "red" clusters, even taking into account the claimed photometric errors, in the range of 0.05–0.15 mag, depending on the cluster location and the source of the photometry.

2.2. *Blue versus Red GCs: An Overall Preliminary Comparison*

Besides the obvious difference in color, it is interesting to further investigate how sample A clusters are characterized as compared to the remaining fraction of red M31 GCs. We therefore extended our analysis to different positional, morphological, and spectrophotometric parameters, according to the BRC data. The left panels of Figure 3 summarize the most striking differences between the two cluster populations. The four histograms report the cluster distribution in absolute V magnitude, in two spectrophotometric indices, namely, the Brodie & Hanes (1986) Δ and the Lick Hβ index (according to the original definition of Faber et al. 1985), and finally in the $W_{1/4}$ structural parameter measured in a homogeneous way by Buonanno et al. (1982) and Battistini et al. (1987) for almost all the M31 cluster candidates.

In the plots, the absolute V magnitudes from the BRC are the result of a full revision of all the available photometry, includ-

ing the *HST* data (see Galleti et al. 2004 for details). Magnitude differences with respect to the extended database of Barmby et al. (2000) are typically less than ± 0.2 mag, depending in general on a different reddening correction, but with no systematic trend of magnitude residuals with GC color.

Both narrowband indices considered in Figure 3 have been taken from Perrett et al. (2002);[10] as a result of their unfluxed observations, however, the instrumental output had to be reduced to a standard system. This has been done relying on a set of 41 M31 GCs in common with Brodie & Huchra (1990) for which both Δ and standard Lick indices are provided in the appropriate units (see Fig. 4). As for Hβ, which measures the strength of the Balmer absorption line in pseudo–equivalent width, we verified that no transformation was necessary for the Perrett et al. (2002) original data, which roughly matched the Lick standard system within a high but still convenient 0.9 Å rms. In the case of the Δ index, measuring the amplitude of the 4000 Å Balmer jump in the integrated spectra of the clusters, the Brodie & Hanes (1986) standard system was reproduced via a linear transformation in the form

$$\Delta_{std} = 0.66\Delta_{Perrett} - 0.3 \text{ mag}, \quad (1)$$

with a 0.12 mag rms in the individual point scatter. The corresponding plots in Figure 3 have been corrected to the standard system accordingly. While spectral index estimates based on spectra of higher quality with respect to those used by Perrett et al. (2002) are available in the literature for small samples of M31 clusters (see, e.g., Burstein et al. 2004), we preferred to rely on a single large and homogeneous data set for our analysis, namely, the one by Perrett et al.

---

[10] Perrett et al. (2002) report all indices in magnitude scale. For the case of Hβ, a transformation to pseudo–equivalent width units (in Å) has been done through the equation $EW = 27.5(1 - 10^{-0.4I})$ (see, e.g., Brodie & Huchra 1990), where I is the original index in magnitude scale.
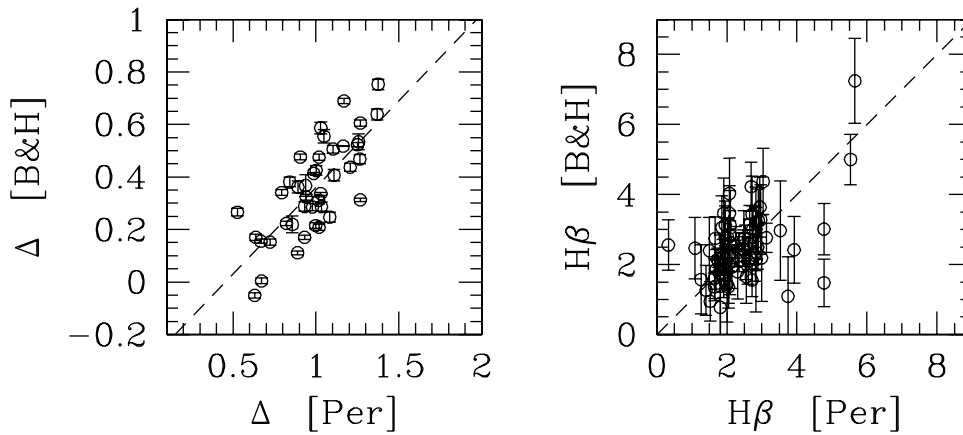
Fig. 4.—Standard calibration for the Brodie & Hanes (1986) Δ and Lick Hβ indices. Data for 41 M31 GCs of Perrett et al. (2002) in common with Brodie & Huchra (1990) are compared, and the least-squares equations of transformation are derived, as labeled in the plots. Note that the Perrett et al. (2002) Hβ index has been converted to pseudo–equivalent width in Å, while the 4000 Å Balmer jump index, Δ, is expressed in magnitudes.

Finally, the bottom histogram of Figure 3 reports the distribution of the Battistini et al. (1980, 1987) $W_{1/4}$ morphological parameter, which nicely relates to the cluster core radius through a fitting King profile (see Battistini et al. 1982 for further discussion). The adopted morphological parameter is obtained from ground-based data; hence, it is likely affected by large uncertainties. However, $W_{1/4}$ estimates are available for a large sample of M31 clusters, and they broadly correlate with the core radii (r_c) estimated from *HST* photometry (see Barmby et al. 2002 and references therein). In particular, *HST*-based estimates of r_c are available for only eight of the 67 clusters listed in Table 1. It is interesting to note that the average core radius for these eight BLCCs is $\langle r_c \rangle = 0''.46$, with a standard deviation $\sigma = 0''.30$, while for 31 non-BLCC confirmed clusters we find $\langle r_c \rangle = 0''.21$ and $\sigma = 0''.12$. Hence, the sparse *HST* data available confirm the trend shown in the lower panels of Figure 3, i.e., BLCCs are larger on average than ordinary GCs.

A Kolmogorov-Smirnov test on the data distribution of the left panels of Figure 3 indicates, at a confidence level better than 99.99%, that sample A BLCCs differ from the remaining fraction of M31 clusters under all the considered aspects. Compared to the GC general distribution, BLCCs are intrinsically fainter and morphologically less concentrated, with a shallower Balmer jump.

The most striking feature, however, is the intensity of the Hβ absorption line, which is much stronger in BLCCs and essentially out of the range covered by ordinary GCs. This is strongly suggestive of young ages, as we discuss in better detail in the next sections.

2.3. A Different (and Complementary) Selection: The Hβ Index

The claimed Hβ enhancement for BLCC candidates opens our analysis to a complementary selection criterion that, relying on this narrowband spectrophotometric index, basically overcomes any problem dealing with the (poorly known) reddening correction for M31 GCs. The peculiar strength of Hβ absorption in the spectra of several M31 GCs is a well-known feature, discussed since long ago by Burstein et al. (1984), Tripicco (1989), Buzzoni et al. (1994), Lee et al. (2000), Peterson et al. (2003), and Schiavon et al. (2004), among others. Since homogeneous Hβ-values are available for most of the M31 clusters from the Perrett et al. (2002) database, one could self-consistently rely on this parameter for a more effective diagnostic of BLCCs.

Similar to the color-selected BLCC sample, on the basis of the observed distribution of Figure 3, we could try a new sample selection, choosing BLCCs as objects with a Lick index H$\beta \geq 3.5$ Å (see Figs. 7 and 8 below). According to this different criterion, a larger number of clusters (51 in total, with 25 objects in common with the color-selected sample A) are included in our bona fide BLCC data set. This is our sample B, as reported in Table 1 and labeled accordingly in the second to last column.

Among the 45 objects in Table 1 with complete $B - V$ and Hβ photometry, only one sample A cluster should not be comprised in the Hβ-selected sample B [this is B206-D048, with $(B - V)_0 = 0.12$ and H$\beta = 2.53$ Å], while 19 sample B clusters are too red in $B - V$ to be included in sample A (thus confirming the presence of a possibly important fraction of strongly reddened young clusters in the M31 GC population).

The right panels of Figure 3 complete the comparison between sample A and B properties in the different parameter domains. The substantial similarity of the two plots and the sharper characterization of the bona fide BLCC candidates in the Hβ-selected sample make the latter spectroscopic selection much more safe and efficient in identifying the *same* kind of clusters than selecting according to the color criterion alone.

2.4. The Final Adopted BLCC Samples

From the previous arguments, from now on we adopt the two samples defined above and analyze sample A and B objects in parallel. Full information for these 67 clusters is summarized in Table 1. In particular, photometry and positional data in the table are from the BRC (unless otherwise stated), [Fe/H], radial velocity, and spectroscopic indices Hβ and Δ are from Perrett et al. (2002) (the latter are converted according to Fig. 4), the morphological parameter $W_{1/4}$ is from Buonanno et al. (1982) and Battistini et al. (1987), and the δ kinematic residuals are from Morrison et al. (2004).

As we already stressed before, a color selection such as that for sample A favors a plain observational approach (90% of the objects in Table 1 have a measured $B - V$, while for only 78% is Hβ provided from spectroscopy), although it is prone to any uncertainty in the reddening correction; on the other hand, Hβ selection, such as in sample B, likely provides a more confident and physical BLCC selection but suffers from more difficult observing constraints. Quite importantly, however, we show that, disregarding any preferred selection criterion, the same conclusions hold for both samples.

TABLE 2
OTHER CONFIRMED AND REPORTEDLY YOUNG M31 GCs

Name	V	$B - V$	$U - B$	$\langle[Fe/H]\rangle$	Δ (mag)	$H\beta$ (Å)	$W_{1/4}$	V_r (km s^{-1})	δ	X (arcmin)	Y (arcmin)	References
B015-V204	17.79	1.41	...	-0.35 ± 0.96	...	-0.54	5.56	-460	-0.04	-26.56	7.91	1
B030-G091	17.39	1.93	0.71	-0.39 ± 0.36	...	1.62	4.69	-380	1.62	-24.83	1.24	1
B090	18.80	...	...	-1.39 ± 0.80	...	3.28	4.62	-428	-0.43	-13.12	-4.60	1
B101-G164	16.87	0.81	0.38	...	...	...	4.49	...	...	-8.01	-2.55	1
B102	16.58	0.62	-0.12	-1.57 ± 0.10	0.224	2.74	3.98	-236	0.17	12.67	13.29	2
B117-G176	16.34	0.65	0.45	-1.33 ± 0.45	0.266	2.70	4.76	-531	-2.68	-16.19	-10.13	3
B146	16.95	1.49	-0.54	...	...	...	4.86	...	...	1.51	-3.23	1
B154-G208	16.82	1.32	0.55	...	...	...	4.95	...	...	3.17	-4.21	1
B164-V253	17.94	1.04	...	-0.09 ± 0.40	0.559	1.48	4.74	-294	0.07	1.00	-7.25	1
B197-G247	17.63	1.08	0.19	-0.43 ± 0.36	...	1.14	4.94	-9	1.30	18.58	-1.06	1
B214-G265	17.65	0.61	0.28	-1.00 ± 0.61	...	3.24	4.90	-258	-1.26	17.19	-5.53	2
B232-G286	15.67	0.72	0.10	-1.83 ± 0.14	0.242	3.13	4.73	-179	2.52	12.52	-17.88	4
B292-G010	16.99	0.90	-0.02	...	...	...	5.30	...	...	-58.32	47.44	5
B311-G033	15.44	0.96	0.14	-1.96 ± 0.07	0.120	2.72	4.53	-463	2.15	-57.58	1.24	4
B324-G051[a]	16.91	0.66	0.79	...	...	...	4.87	...	...	3.10	36.44	3, 4, 5
B328-G054	17.86	0.89	0.48	...	...	...	5.44	...	...	3.20	35.57	1, 2
B347-G154	16.50	0.73	0.15	...	...	...	5.16	...	...	27.83	26.66	3, 4
B423	17.72	0.60	0.10	...	...	...	6.33	...	...	-47.66	31.80	2
B468	17.79	0.70	...	...	...	...	7.52	...	...	-66.43	-58.30	2
NB 16	17.55	0.66	...	-1.36 ± 0.12	...	...	...	-115	1.35	1.97	4.21	3
B150D	17.55	0.61	-0.04	...	...	...	...	...	...	-31.77	57.17	2

[a] Photometry from Sharov et al. (1995).

REFERENCES.—(1) Jiang et al. 2003; (2) Barmby et al. 2000; (3) Barmby & Huchra 2001; (4) Burstein et al. 2004; (5) Beasley et al. 2004.

As a final remark about our sample selection, we should also note that a number of other BLCC candidates (confirmed or not) have been picked up by various authors based on different observations and procedures. For the sake of completeness, we have carried out an exhaustive search in the M31 literature, assembling a coarser set of reportedly "young" objects and listing our results in Table 2 (21 confirmed GCs) and Table 3 (69 GC candidates to be confirmed), together with the corresponding reference studies.[11]

In the present analysis, however, we restrain ourselves to only the bona fide samples (i.e., Table 1 data), postponing to a future paper a complete review of each individual object.

3. DYNAMICS AND DISTINCTIVE PHYSICAL PROPERTIES OF BLCCs

After a thorough analysis of the positional and kinematic properties of M31 GCs, based on the Perrett et al. (2002) data, Morrison et al. (2004) concluded that the GCs in this galaxy belong to two kinematic components: ". . . a thin, rapidly rotating disk . . . and a higher velocity dispersion component whose properties resemble that of M31's bulge." According to these authors, membership in one of the two dynamical components is assessed for each cluster on the basis of its residual velocity with respect to a disk model, choosing disk clusters as those with residual $|\delta| < 0.75$ (in normalized units; see Morrison et al. 2004). The claimed probability of misclassification with this procedure turns to be about 30%.

3.1. The Morrison et al. (2004) Framework and the Spatial and Kinematic Properties of BLCCs

In Figure 5 we compare the spatial distribution (in the X and Y projected distances along the major and minor axes, respec-

tively) and the V_r versus X distribution of sample A (left panels) and B (right panels) BLCC candidates with the remaining fraction of "ordinary" M31 GCs. The thin plot of points in the X-Y panels mainly maps the brightest asymptotic giant branch (AGB) and carbon stars of M31 from the Two Micron All Sky Survey (2MASS) Point Source Catalog (Cutri et al. 2003)[12] and therefore gives a neat picture of the outermost structure of the galaxy disk (van den Bergh 2000; Hodge 1992), allowing us to appreciate in some detail the overplotted GC distribution.

It is evident from the figure that ordinary clusters (Fig. 5, top panels) are uniformly distributed all over the apparent body of M31, up to distances of $X \simeq 100'$ ($d \simeq 22$ kpc) from the galaxy center, closely tracing the smooth luminosity profile of M31. In addition, most of the bulge clusters show a clear sign of coherent rotation in the V_r-X plane, as a part of the rotationally supported structure of the galaxy (Morrison et al. 2004). However, the large scatter around the overplotted rotation curve (taken from van den Bergh 2000, Fig. 3.10), indicates that pressure support has a significant role in the overall kinematics of the sample (see, however, Morrison et al. [2004] for a deeper analysis of these clusters).

On the contrary, BLCCs seem to avoid the inner regions of the galaxy (see Fig. 5, bottom panels) and appear well projected onto the outer disk, with a strong correlation with the underlying spiral substructures. Also, the velocity pattern traces the velocity curve of the disk quite well.

Our conclusion, therefore, is that both color-selected and $H\beta$-selected BLCCs belong to the cold thin disk of M31, in agreement with the previous results of Beasley et al. (2004) and Burstein et al. (2004), which were limited, however, to a much smaller subset of clusters.

To further clarify this issue, in the top panels of Figure 6 we plotted the Morrison et al. (2004) residuals (taken from Table 2 therein), singling out our bona fide BLCCs. It is quite evident

[11] Data sources for the Table 2 and 3 entries are the same as for Table 1 unless explicitly reported. Note, of course, that for Table 3 targets one would require a clear-cut spectroscopic check because of a possibly high contamination by spurious objects.

[12] The 2MASS sources with color and magnitude constraints such as $1.3 \leq J - K_S \leq 2.0$ and $14.0 \leq K_S \leq 15.7$ have been selected to better tune in on the M31 stellar population.

TABLE 3

UNCONFIRMED M31 GCs AND REPORTEDLY YOUNG AND/OR POSSIBLE CANDIDATE BLCCs WITH $(B - V)_0 < 0.45$

Name	V	$B - V$	$U - B$	X (arcmin)	Y (arcmin)	References
B060-G121......................	16.75	0.71	0.08	−14.10	0.38	1
B070-G133......................	17.07	0.54	0.19	−10.83	0.56	
B089..............................	18.18	0.10	−0.32	16.05	17.93	1
B100-G163......................	17.91	0.88	0.15	−22.53	−13.75	1
B108-G167......................	17.47	0.89	1.01	−7.30	−2.49	1, 2
B145..............................	18.10	0.32	1.48	−0.95	−4.82	1, 3
B150-G203......................	16.80	1.10	0.39	5.97	−0.87	2
B157-G212......................	17.73	0.65	−0.11	−0.39	−7.36	1
B173-G224......................	18.27	0.02	. . .	10.21	−2.61	
B192-G242......................	18.28	0.20	0.32	23.73	4.21	1, 2
B195..............................	18.57	0.40	0.97	−3.39	−17.95	1
B323..............................	17.59	0.47	0.17	−51.25	−4.57	
B330-G056......................	17.72	0.95	0.09	5.33	36.93	4
B362..............................	17.61	0.65	0.08	29.90	3.14	2
B371-G303......................	17.54	0.48	0.39	40.53	−7.04	1
B414..............................	17.98	0.50	0.08	4.58	93.72	
B442-D033......................	17.94	0.39	0.16	−47.36	−1.87	1
B452-G069......................	17.78	0.38	−0.05	−45.89	−7.66	1
B460..............................	18.35	0.54	−0.23	−85.52	−54.13	
B469-G220......................	17.58	0.53	−0.04	46.76	28.06	1, 4
B477-D075......................	18.46	0.32	. . .	35.11	−6.78	
B508..............................	17.12	0.46	0.27	54.77	−57.54	
B190D-G048...................	18.17	0.24	−0.29	−46.03	−0.26	
G085-V015	17.39	0.23	0.05	−43.73	−11.86	
B028D-G100...................	18.04	0.40	−0.21	−26.71	−4.77	
G137..............................	17.81	−0.02	−1.16	5.75	12.76	
G270..............................	17.30	0.46	−0.77	23.70	−2.39	
H126..............................	16.76	0.42	−0.03	43.75	13.32	
NB 39-AU 6	17.94	0.21	0.40	0.18	−0.79	
NB 42............................	18.49	0.52	. . .	1.49	0.56	
NB 47-AU 3	18.75	0.10	. . .	1.44	3.59	
B065D-NB69	16.83	0.37	. . .	1.41	2.52	
NB 79............................	18.27	0.53	. . .	−2.87	2.01	
NB 107..........................	18.65	0.31	. . .	−2.28	1.62	
B134D...........................	18.19	0.46	−0.19	−74.79	46.10	
B137D...........................	18.51	0.54	−0.05	−59.80	45.32	
B139D...........................	18.59	0.44	. . .	−116.18	2.35	
B147D...........................	17.96	0.49	−0.44	−47.16	49.24	
B158D...........................	16.50	0.33	0.02	−103.80	−5.69	
B162D...........................	17.85	0.44	−0.52	−91.16	−0.17	
B171D...........................	17.80	0.43	0.08	−57.63	14.65	
B173D...........................	17.45	0.55	−0.43	−54.91	15.16	
B196D...........................	18.79	−0.21	−0.94	−54.20	−10.79	
B216D...........................	18.21	0.30	0.01	28.36	21.50	
B218D...........................	18.19	0.44	−0.02	41.70	28.85	
B220D...........................	16.94	0.53	−0.06	−65.70	−55.73	
B225D...........................	18.15	0.50	−0.19	−55.82	−50.27	
B227D...........................	16.91	−0.01	0.03	−44.15	−41.65	
B246D...........................	18.05	0.09	−0.77	49.50	15.14	
B253D...........................	17.68	0.53	0.03	−16.92	−42.36	
B261D...........................	17.60	0.46	−0.04	60.74	11.30	
B270D...........................	17.50	0.40	0.34	10.14	−36.21	
B272D...........................	16.34	0.51	0.37	−24.27	−64.72	
B286D...........................	17.76	0.47	−0.91	−7.48	−59.92	
B293D...........................	17.91	0.54	−0.12	−29.58	−81.90	
B303D...........................	18.27	0.31	0.91	−43.52	−97.03	
B312D...........................	18.35	0.53	. . .	−24.72	−88.18	
B320D...........................	17.78	0.45	−0.56	72.08	−13.85	
B322D...........................	18.26	0.17	0.29	−36.49	−101.57	
B324D...........................	18.74	0.55	−0.03	58.96	−27.38	

TABLE 3—*Continued*

Name	V	B − V	U − B	X (arcmin)	Y (arcmin)	References
DAO 46[a]	18.75	0.53	. . .	−47.09	−16.89	1
DAO 52	18.42	0.14	−0.50	−24.11	−10.15	1
DAO 69[a]	17.48	0.26	. . .	42.11	6.66	1
V014	17.39	0.35	0.04	−43.86	−12.20	5
V034	17.48	0.13	−1.15	−17.30	4.24	
V133	18.36	0.06	−1.26	51.54	5.58	
V270	18.07	0.27	−0.67	12.26	9.93	
SH 06	16.54	0.28	−0.71	−27.99	27.16	
BH 02	18.50	0.40	. . .	−49.25	−1.15	

[a] Photometry from Barmby et al. (2000).
REFERENCES.—(1) Barmby et al. 2000; (2) Jiang et al. 2003; (3) Bohlin et al. 1993; (4) Elson & Walterbos 1988; (5) van den Bergh 1967.

from the plots that BLCCs stand out naturally as a very low-δ family. Almost the whole BLCC population (independent of the adopted selection), in fact, matches the Morrison et al. (2004) disk-membership criterion, and only a few such clusters exceed $|\delta| > 1.5$. This feature is also summarized in the bottom panels of Figure 6, in which the hatched histograms give the residual distributions of BLCCs compared to the whole sample of ordinary GCs. Complementing the Morrison et al. (2004) results, we can conclude the following:

1. Both color- and Hβ-selected BLCCs can effectively comprise a significant fraction of "disk clusters," natural tracers of the cold, thin disk subsystem of M31 (Morrison et al. 2004; but see also Burstein et al. 2004).

2. BLCCs appear to constitute a separate family for what concerns a number of nonkinematic properties, such as, for instance, the absolute magnitudes, the Hβ and Δ indices (at least), and the structural parameters.

3.2. *The Hβ and Δ Indices as Age Tracers*

In a quite common view, a blue integrated color for a cluster is actually an indication of a young age, as its integrated color is dominated by the bright blue stars at the MSTO point. On this basis, even early studies of M31 clusters (see, e.g., van den Bergh 1967, 1969) immediately noticed that most of the blue cluster candidates should be young. The combined information provided by Hβ and the Balmer jump, Δ, allows us in principle to tackle the problem of dating BLCCs in finer detail; both indices, in fact, are contributed to by the warmer stellar component in a simple stellar population (SSP) and can selectively probe the MSTO temperature location (Buzzoni 1995a, 1995b), therefore leading to an indirect estimate of age in a stellar aggregate.

Note that, because of its photometric characteristics, the Δ index recalls to some extent the broadband $U − B$ color, but its narrower wavelength baseline makes the Brodie & Hanes

Sample "A" Sample "B"
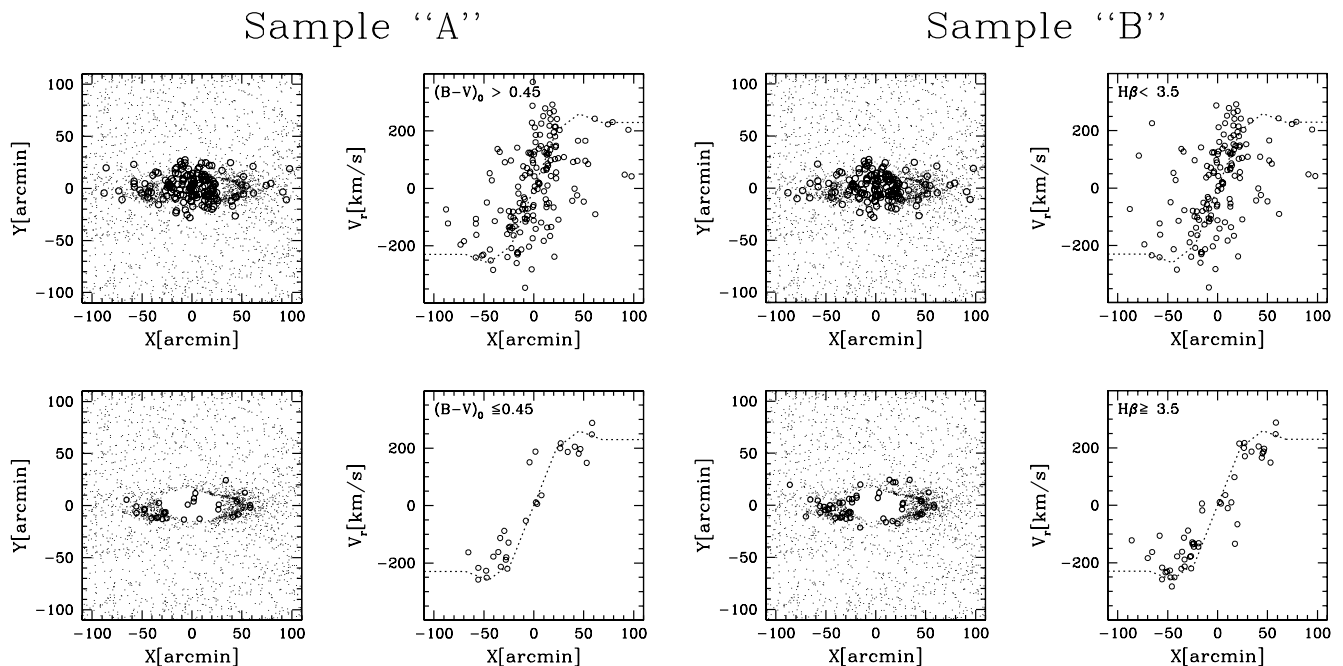
FIG. 5.—Spatial distribution and kinematic properties of M31 ordinary GCs, with $(B − V)_0 > 0.45$ or H$\beta < 3.5$ Å, as labeled (*top panels*), compared with the BLCCs of samples A and B (*bottom panels*). The smoothed disk structure in the M31 maps is traced by the PSC 2MASS sources (Cutri et al. 2003), mainly consisting of bright AGB members and carbon stars. Overplotted on the radial velocity distribution, as a function of the major axis displacement X, is the rotation curve of the M31 disk according to van den Bergh (2000).
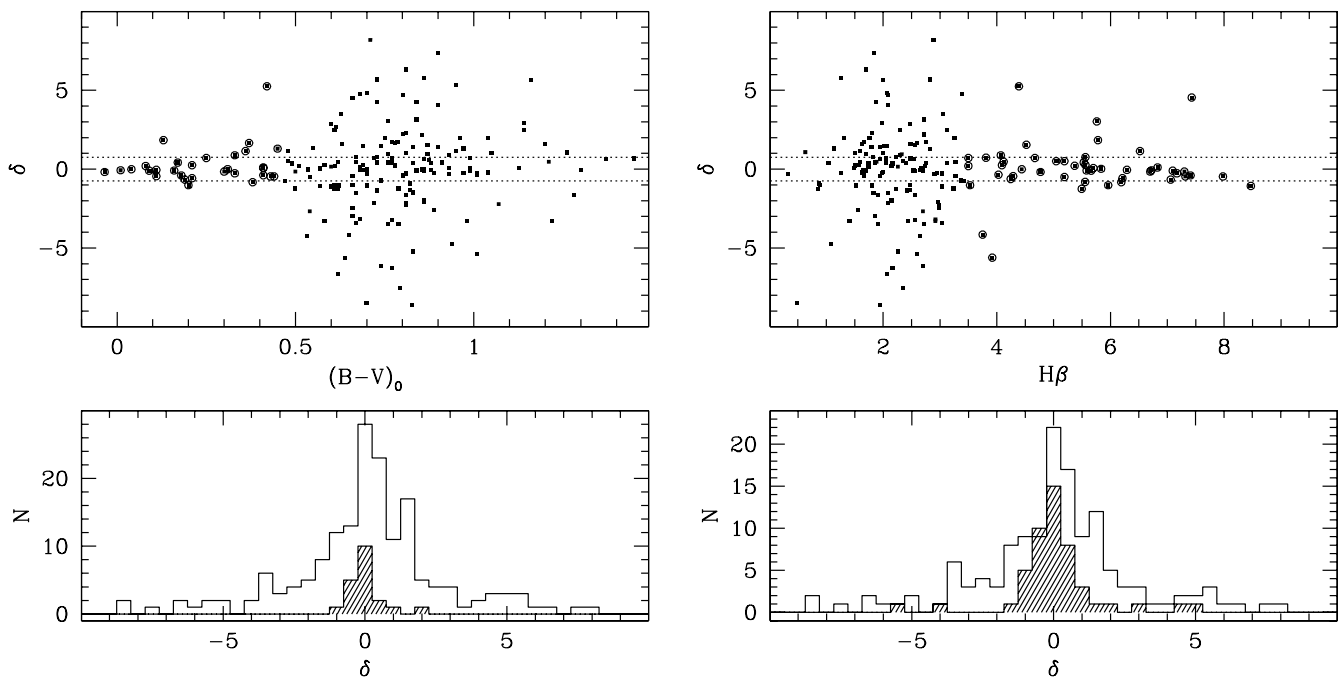
Fig. 6.—GC kinematic residuals δ with respect to the Morrison et al. (2004) disk model for M31. The BLCC distribution, according to samples A (*top left*) and B (*top right*), is marked on the plots (*large circles*) with the remaining fraction of ordinary clusters (*squares*). The dotted lines enclose the low-residual region with $|\delta| \leq 0.75$ (such low-δ clusters basically share the disk kinematics, according to the model of Morrison et al.). The histogram of the δ-distribution for each plot is also summarized in the bottom panels for BLCCs (*hatched histograms*) and ordinary GCs (*open histograms*).

(1986) index much less sensitive to the reddening, and therefore a better tracer of the intrinsic properties of a stellar cluster.[13]

Figure 7 is our reference plot to summarize the main features of an Hβ-Δ diagram, from the theoretical point of view. In the figure we report the expected locus for MS stars of different temperatures, up to $T_{\rm eff} = 50,000$ K, and their inferred spectral types according to the Johnson (1966) calibration, as labeled.

Our calculations rely on the new BLUERED theoretical library of stellar spectral energy distributions (SEDs; Bertone 2001; Bertone et al. 2003), from which we extracted a grid of model atmospheres with $\log g = 3$ and 5 and $[\rm Fe/H] = -2.0$, -1.0, and solar. The vanishing sensitivity of both spectral indices to the contribution of late-type stars makes the Hβ versus Δ information nearly independent of the exact post-MS details of the color-magnitude diagram. This allows a very immediate and straightforward comparison of the theoretical stellar locus with the integrated indices of BLCCs, providing a first effective constraint to the age through MSTO calibration linking: $T_{\rm eff} \rightarrow M_{\rm MSTO} \rightarrow t_{\rm MS}$ (see, e.g., Buzzoni 2002).

In a more elaborate scheme relying on SSP models, however, one should also account for the supplementary contribution of blue HB stars, which are expected to play a role at some stage of late evolution of low-mass stars modulating the integrated SED of old stellar populations, typically beyond 10 Gyr. A more accurate prediction of the integrated output for SSPs of different metallicity and HB morphology is reported in Figure 7, based on the Buzzoni (1989)[14] population synthesis models.

The effect of HB morphology is sketched for the 15 Gyr SSP models, mainly resulting in a sensible enhancement of the Hβ
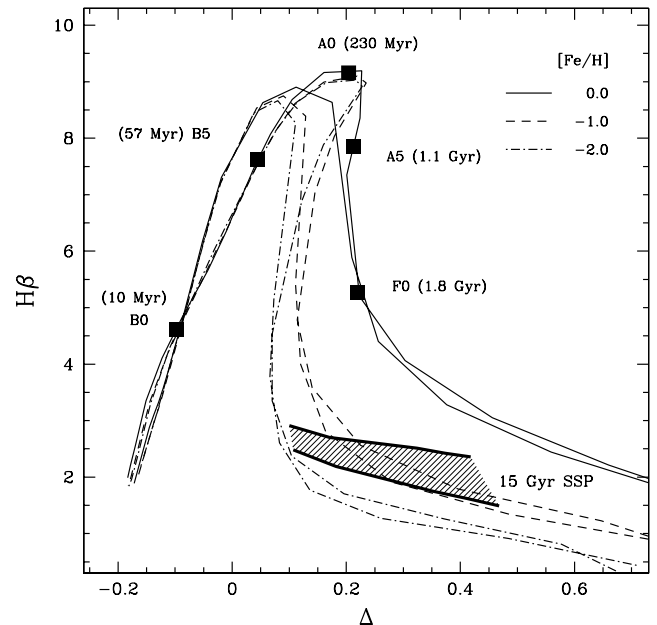
Fig. 7.—Theoretical diagram for the Hβ Lick index (in Å) vs. the Balmer jump Δ index (in magnitude scale). Thin curves are the expected locus for MK V stars of different temperatures, from 5000 to 50,000 K, surface gravity ($\log g = 4$ and 5, the latter being the shelf of curves peaking at slightly higher values of Hβ), and metallicity (from $[\rm Fe/H] = -2$ to solar, as labeled). Theoretical indices rely on the BLUERED library of synthetic stellar spectra (Bertone 2001; Bertone et al. 2003). The empirical spectral type vs. effective temperature calibration of Johnson (1966) is marked on the ($\log g$, $[\rm Fe/H]$) = (5, 0.0) curve, together with the estimated MS lifetime of stars, as derived from Buzzoni (2002). The hatched area is the region for the 15 Gyr SSP models of Buzzoni (1989), with a different HB morphology. The lower edge of the area is for a red-clump HB morphology, while the upper edge is for a blue HB. SSP metallicity spans the range $[\rm Fe/H] = -2.27$ to $+0.22$ dex, in the sense of increasing Δ.

---

[13] The Brodie & Hanes (1986) Δ index is defined in a magnitude scale as $\Delta = 2.5 \log (F2/F1)$, where $F1$ and $F2$ are the luminosity densities (per unit wavelength) in two 200 Å wide bands centered at 3900 and 4100 Å, respectively. This has to be compared with the Johnson U and B bands, centered respectively at 3600 and 4400 Å. According to Scheffler's (1982) compilation, the expected color excess can be computed as $E(\Delta)/E(U - B) = 0.25$ and $E(\Delta)/E(B - V) = 0.18$.

[14] See also http://www.bo.astro.it/~eps/home.html for the latest model update.
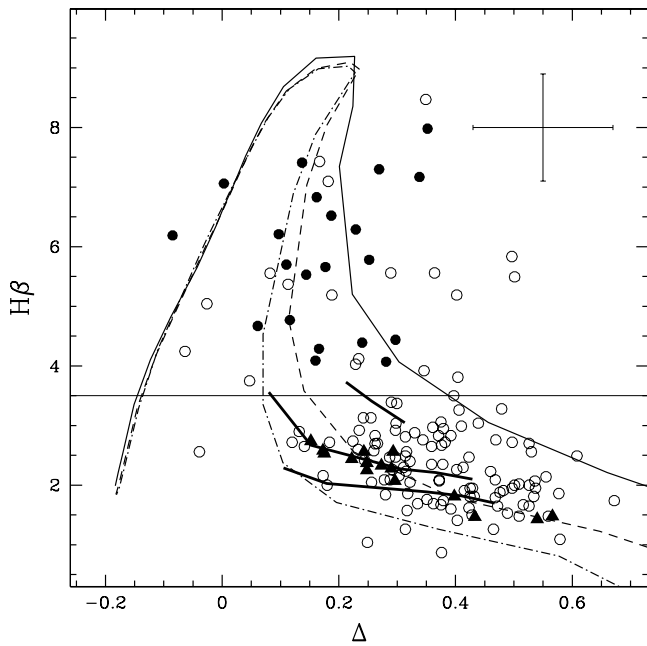
Fig. 8.—M31 GC distribution in the Hβ vs. Δ index plane. Reference curves for log g = 5 stars of different temperature (from 5000 to 50,000 K) and metallicity ([Fe/H] from -2 to solar) are reported from Fig. 7. Sample A (i.e., color-selected) BLCCs are singled out (*filled circles*). By definition, sample B comprises all the targets in the plot above the Hβ = 3.5 Å threshold, as marked (40 objects with available indices from Table 1). For comparison, triangles show the Brodie & Huchra (1990) data for MW GCs, while thick solid lines are the locus for the Buzzoni (1989) SSP models with t = 15, 8, and 2 Gyr (in the sense of increasing Hβ), red HB morphology, and metallicity [Fe/H] = -2.27 to +0.22. Typical error bars for M31 data are shown at the top right.

Fig. 9.—M31 GC distribution in the Hβ vs. (dereddened) $U - B$ index plane. As in Fig. 8, sample A BLCCs are shown by filled circles, while, by definition, sample B comprises all the objects with H$\beta \geq 3.5$ Å. The four panels report a comparison with SSP models from different population synthesis codes: Buzzoni (1989; for t = 15, 8, and 2 Gyr; *top left*), Bruzual & Charlot (2003; for t = 15, 2, 1, and 0.1 Gyr; *top right*), Kurth et al. (1999; for t = 15, 2, and 1 Gyr; *bottom left*), and Worthey (1994; for t = 12, 8, and 2 Gyr; *bottom right*). In all cases, the synthetic Hβ index increases with age (excepting the 100 Myr model of Bruzual & Charlot [2003], with a negative $U - B$ and a "fading" Hβ index, recalling the trend of Fig. 7).

strength. It is clear, however, that in no cases could the late evolutionary scenario account for very strong Hβ-lined clusters (i.e., H$\beta \gtrsim 3.0$ Å), where a prevailing contribution of F-type stars calls for a genuinely blue MSTO, and therefore for a young age, certainly less than a few gigayears.

The distribution of M31 GCs in the Hβ-Δ plane is displayed in Figure 8. Filled circles show the 21 sample A BLCCs from Table 1 with available Hβ and Δ indices (by definition, sample B comprises all 40 filled and open circles above the Hβ = 3.5 Å threshold, as indicated in the figure). The MW GC data from Brodie & Huchra (1990) (*triangles*) are also reported for comparison. The stellar loci of Figure 7 (only those for log g = 5 and different metallicity, for the sake of clarity) have also been overplotted, together with the SSP locus for different ages (and a red HB morphology), according to Buzzoni (1989).

It is evident from the figure that, while the bulk of ordinary GCs (including the MW GCs) have spectral properties consistent with an age of several gigayears, the BLCC indices are clearly dominated by a younger stellar component of A–F stars of moderately high metallicity (mostly solar or slightly sub-solar). This places a confident upper limit to BLCC ages of $\sim$2 Gyr. Note also (Fig. 8) that only four of the 40 BLCCs lie on the branch of the theoretical stellar loci typical of ages lower than $\sim$50 Myr ($\Delta < 0.0$), while the bulk of the population is consistent with ages larger than $\sim$200 Myr.

3.2.1. *The (U − B) Color As an Alternative to the Δ Index*

As we commented in § 3.2, a more standard assessment of the BLCC distribution with respect to the overall GC population in M31 can be carried out relying on the $U - B$ color. For the nature of the population, this choice would allow a more comfortable match with the theoretical output of population synthesis models
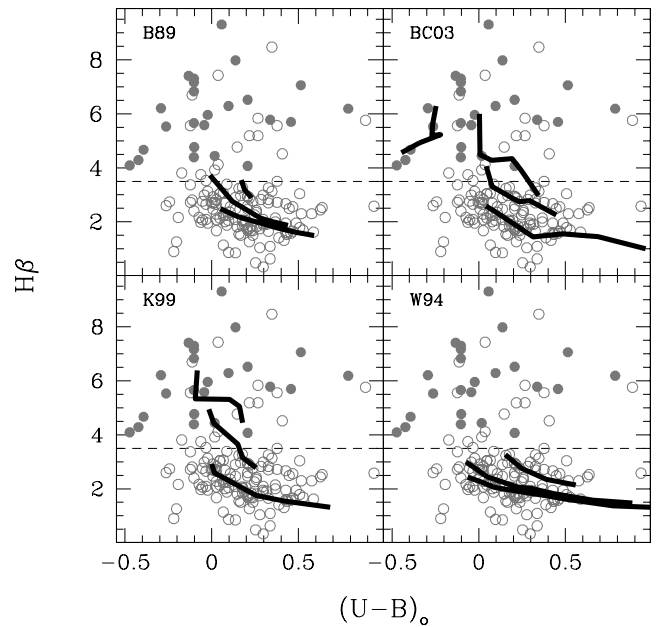
and would certainly ease the inclusion of a larger GC database with available data, although observations are obviously more critically plagued by reddening uncertainty (see footnote 13).

In Figure 9 the M31 (dereddened) data are compared with the expected SSP evolution according to four different population synthesis codes, namely, those of Buzzoni (1989; and further Web updates), Worthey (1994), Kurth et al. (1999), and Bruzual & Charlot (2003). Again, models agree in the overall classification scheme, with the age of Hβ-poor GCs fully consistent with old (i.e., 10–15 Gyr) evolutionary scenarios and BLCCs better matched by young ($t \lesssim 2$ Gyr) SSPs.[15]

The emerging evidence, from the combined analysis of the BLCC age range (Figs. 8 and 9) coupled with the kinematic information of Figure 5, leads eventually to the important conclusion that over 25% of the Perrett et al. (2002) sample (that is, at least 15% of the whole sample of confirmed M31 clusters) consists of young BLCCs, located in the outskirts of the thin disk of M31 and sharing the kinematic properties of this galactic component. This global evidence is quite new and points to the existence of a significant difference between the M31 and MW GC systems, which may have deep implications on the understanding of formation and evolution of the two parent galaxies.

3.3. *Metallicity: BLCCs Might Not Be As Metal-poor As Claimed*

Another important issue in the Morrison et al. (2004) discussion concerns the claimed similarity of "disk" and "bulge"

---

[15] In this framework, the peculiar case of B206-D048, i.e., the only sample A cluster not in the BLCC Hβ selection (see § 2.3), might be indicating an old and very metal-poor stellar population. This interesting cluster does not appear in Figs. 8 and 9, as it lacks $U - B$ and Δ indices (see Table 1).
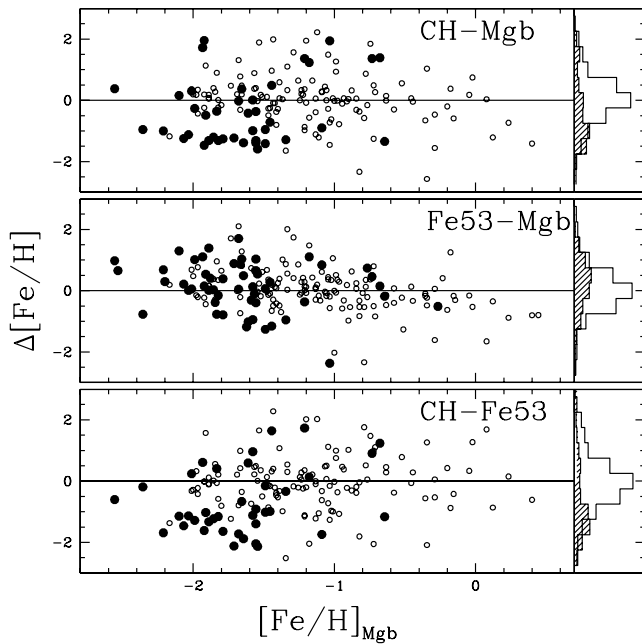
Fig. 10.—Metallicity estimates from single Lick spectrophotometric indices for M31 GCs according to Perrett et al. (2002). Reported are the differences in the inferred value of [Fe/H] for each individual cluster from the empirical calibration of the CH (G band), Mg b, and Fe5335 indices. Sample B BLCCs are shown by filled circles, while Δ[Fe/H] residual distribution is summarized by the vertical histograms on the right (hatched for BLCC distribution and open for the remaining GC population). For BLCCs a systematic bias on the average estimate of [Fe/H] (reported in Table 1) induced by the exceedingly metal-poor abundance inferred by the G band (Δ[Fe/H] $\simeq -1$ dex; cf. top and bottom panels in the figure) is evident. Both Mg b and Fe5335 metallicity values are, on the contrary, fully self-consistent on average (cf. middle panel).

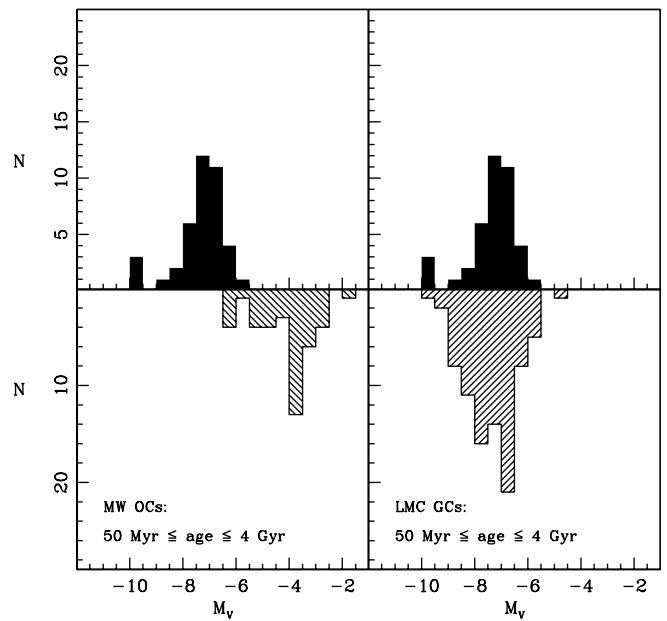

Fig. 11.—Comparison of the LF of the M31 BLCCs (top panels, filled histograms) with the LF of the OCs of the MW in the same age range (bottom left) and the LF of the LMC GCs in the same age range (bottom right).

GC metallicity that, as in the MW, should be regarded as a striking sign of coevality for the whole GC population in M31. In fact, if our bona fide BLCCs were mostly metal-poor, as apparently deduced from the metallicity values reported by Perrett et al. (2002), one would be left with the embarrassing scenario in which the vast majority of the most metal-poor clusters in M31 should be young and likely members of the thin disk galaxy subsystem.

To better assess this issue, one should consider that the Morrison et al. (2004) metallicity scale comes from the Perrett et al. (2002) [Fe/H] estimates, relying on the empirical calibration of three narrowband Lick indices (namely, the G band, Mg b, and Fe5335) from a coarse set of M31 GCs with available [Fe/H] determination from the literature. Given the prevailing contribution of old GCs in this sample, the Perrett et al. (2002) calibration actually introduces a subtly circular bias in the inferred value of [Fe/H] for BLCCs because of the well-recognized age-metallicity degeneracy (Renzini & Buzzoni 1986) that makes young metal-rich clusters resemble old metal-poor ones. This is shown in Figure 10, in which we plot the [Fe/H] difference as inferred from the Lick index determinations for each individual cluster.

From the figure one can immediately recognize a systematic bias induced by the [Fe/H] estimates from the G band. As a matter of fact, while the metallicity scale, as derived from the Fe5335 and Mg b indices, basically agrees on average (see Fig. 10, middle), for the BLCCs (filled circles) the G-band line strength tends to yield a significantly lower (roughly ∼1 dex) value of [Fe/H]. This systematic trend especially affects BLCCs, whose low age mimics the effect of metal deficiency.

In an SSP, this CH molecular feature maximizes its sensitivity to the coolest stars at the tip of the AGB and red giant branch (RGB) (Gorgas et al. 1993; Burstein et al. 1984) and is therefore a mixed age/metallicity indicator, through a composite and complex dependence on the AGB morphology. Conversely, both the Mg and Fe indices are more sensitive to the bulk of stars in the RGB, via chemical opacity, and more confidently trace SSP metallicity (Buzzoni 1995a, 1995b).

As a further argument, we note that even the observed morphology of the Williams & Hodge (2001a) color-magnitude diagrams for the four BLCCs observed so far with HST seem to indicate a metallicity in the range $-0.7 \lesssim$ [Fe/H] $\lesssim 0.0$. This also basically agrees with our "first-look" estimate of [Fe/H] from Figure 8, in which the BLCCs Hβ-Δ distribution suggests a moderately enhanced metallicity (i.e., [Fe/H] $\gtrsim -1.0$ dex).

3.4. BLCCs: Blue Globular Clusters or Massive Open Clusters?

The actual classification of BLCCs as "young globular clusters" or "massive open clusters" is somehow a question of semantics. The real point that is worth investigating is whether these clusters have a counterpart in our own Galaxy, e.g., whether clusters of similar age and luminosity do exist in the MW. While the luminosity range spanned by BLCCs is within that of ordinary GCs, the age distribution of present-day MW GCs is obviously not consistent with the young age of BLCCs. On the other hand, Galactic OCs are comparably young, but they appear less luminous on average than BLCCs.

The LFs of the sample B clusters and the Galactic OCs (data drawn from the WEBDA database; Mermilliod 1995)[16] are compared in Figure 11 (bottom left). The plot shows that Galactic OCs with ages similar to BLCCs are systematically fainter; the two histograms barely overlap. The only Galactic OCs that reach the luminosity range covered by BLCCs are younger than 30 Myr (e.g., they are clusters whose luminosity

---
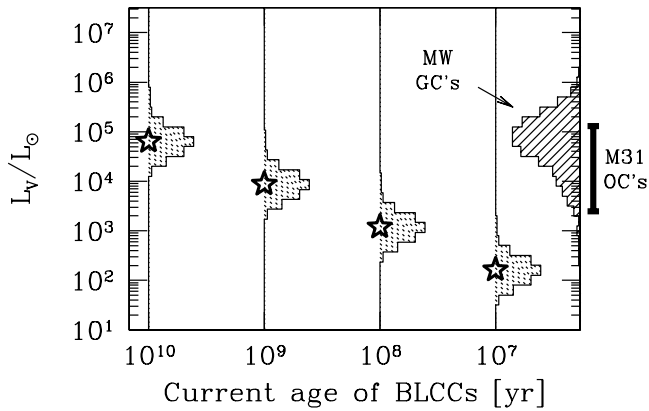
[16] See http://obswww.unige.ch/webda.

FIG. 12.—Effect of evolution on BLCC luminosity. The dotted histograms trace the expected BLCC LF as predicted at $t = 10$ Gyr, according to different values assumed for the current typical age of these objects (as labeled on the *x*-axis). We assume an SSP evolution, according to Buzzoni's (1989) synthesis models for a Salpeter IMF and a (roughly) solar metallicity. For comparison, the observed luminosity distribution of MW GCs is reported on the right vertical axis, derived from Harris (1996) (*hatched histogram*), while the indicative luminosity range for M31 OCs is also sketched (*thick solid bar on the right*) according to Hodge (1979).

budget is dominated by a few massive stars, much different from the BLCCs studied by Williams & Hodge [2001a]), while Figures 7 and 8 above indicate that ≃90% of BLCCs are likely older than ∼200 Gyr. Hence, regardless of the quite high incompleteness that probably still affects the LF of M31 clusters for $M_V \geq -6.0$, the MW lacks OCs as luminous as BLCCs in the proper age range (200 Myr ≤ age ≤ 2 Gyr).

Conversely, Figure 11 (*bottom right*) shows that the luminosity range spanned by M31 BLCCs is very similar to that covered by LMC GCs of similar age (data from van den Bergh [1981]). The above direct evidence leads us to conclude that there is no Galactic counterpart to the young massive M31 clusters studied here; they are much younger than present-day Galactic GCs, and they are much more luminous than present-day Galactic OCs of similar age. On the other hand, BLCC counterparts are quite common in the LMC, as already noted by Burstein et al. (2004). Obviously, this conclusion rests on the age estimates of BLCCs as derived from Figure 8 above. The involved uncertainties leave (formally) open the possibility that several BLCCs have ages less than 50 Myr. If so, they should be interpreted as the counterparts of young OCs of the MW. The availability of a deep color-magnitude diagram is probably the only observational test that can eventually establish the real nature of these objects.

It remains to be explored how BLCCs would appear in the future, in particular, if they would look like classical GCs when they become comparably old. If we assume BLCCs to consist of plain SSPs, then one should expect their luminosity to fade with time, as the stellar population becomes older and photometrically dominated by low-mass stars. In particular, for an SSP of roughly solar metallicity and a Salpeter initial mass function (IMF), evolutionary population synthesis models predict a quite precise luminosity change, such as $L_V \propto t^{-0.9}$, over a wide range of age (e.g., Tinsley & Gunn 1976; Buzzoni 1995a). According to the assumed age of present-day BLCCs, one could infer the expected luminosity of these clusters at $t = 10$ Gyr and more consistently compare with the observed LF of old MW GCs. The results of this illustrative exercise are summarized in Figure 12; it is evident from the figure that, in the more likely case of a current age in the range of 10^8–10^9 yr,

BLCCs would end up at 10^{10} yr populating the low-luminosity (and low-mass) tail of the current MW GC distribution. On the contrary, in the more extreme (and quite unlikely) case of a current age of only a few times 10^7 yr, we would be left at 10 Gyr with extremely faint BLCCs, certainly out of range of the typical MW GCs. Finally, if nowadays BLCCs are already evolved systems (i.e., a few gigayears or older), then at $t = 10$ Gyr their expected luminosity will not change so much, and their distribution would be fully consistent with the bulk of both M31 OCs and MW GCs. A fair assessment of the present-day age distribution of this kind of cluster is therefore a mandatory step to consistently locating them in the appropriate evolutionary framework.

4. DISCUSSION AND SUMMARY

Until a few years ago, the M31 cluster system was commonly viewed as an almost identical (although much larger) analog of the MW GC system, apart from small differences in average metallicity (M31 is about 0.2 dex richer than the MW) and controversial peculiarities in various spectral indices (Burstein et al. 1984, 2004, and references therein). Recent wide-field imaging (Ibata et al. 2004 and references therein), together with high-precision spectroscopy (Perrett et al. 2002; Burstein et al. 2004), have led, however, to a more detailed recognition and investigation of M31 substructures, including its GC system, leaving space for the idea that the Andromeda and MW cluster systems are actually more different than conceived so far.

In particular, Morrison et al. (2004) have put forward a new scenario suggesting the existence in M31 of a quite sizable population of GCs associated with the thin disk and claimed to be old and metal-poor. The natural conclusion from such evidence, if confirmed, is that the thin disk was formed when its oldest metal-poor GCs were in place and that no significant perturbation affected M31, and in particular its thin disk, since then. An in-depth analysis of the claimed thin disk GC members, and in particular of the metal-poor ones, may thus greatly help to clarify this important dynamical issue.

The present study has tackled the problem from a different point of view, i.e., by building up a revised global sample of M31 GCs with intrinsically bluer color than the MW counterparts and assessing whether these bona fide BLCCs (sample A in our analysis) could be further discriminated with respect to "normal" M31 and MW GCs as far as other intrinsic properties (such as absolute magnitude, metallicity, spectral indices, structural parameters, and age) and kinematic behavior are concerned. On the basis of this comparison, a precise and more physical selection based on the Hβ spectral index has been proposed (sample B in the previous discussion). Quite interestingly, both color- and Hβ-selected samples lead to fully consistent conclusions of our analysis.

It has been possible to convincingly demonstrate here that both samples consist of moderately young ($t \lesssim 2$ Gyr) stellar systems, not as metal-poor as previously estimated and basically sharing thin disk kinematics (see also Beasley et al. [2004], in this line of investigation). Since (1) essentially all the blue clusters in the thin disk subsystem as defined by Morrison et al. (2004) are likely young and (2) the metallicity values adopted by these authors are systematically underestimated (at least for most BLCCs; see § 3.3), serious doubts are cast on the actual presence of metal-poor (and old) clusters in the thin disk of M31 as claimed by Morrison et al. (2004).[17] This argument

---

[17] While the present paper was in the peer review phase, a preprint was posted (Puzia et al. 2005) that also develops some of the arguments discussed here.

greatly weakens the possible contrast with the Brown et al. (2003) hypothesis of an equal-mass merging event suffered by M31 6–8 Gyr ago.

Given the evidence presented so far and within the framework discussed above, one might naturally also ask whether the "red" clusters claimed to be members of the M31 thin disk subsystem are actually old and metal-poor (as at least some of them seem to appear) or whether they could display some spread in age and/or metal abundance. The answer to such a question is of paramount importance to settle in finer detail the

mechanisms and formation timescale for the M31 thin disk and for the global evolution of the galaxy system as a whole.

We would like to warmly thank Kathy Perrett for providing us with her full database of M31 GCs in electronic form. This research has been partially supported by the Italian Ministero dell'Universitá e della Ricerca, through COFIN grant 2002028935-001, assigned to the project "Distance and Stellar Populations in the Galaxies of the Local Group."

REFERENCES

Abadi, M. G., Navarro, J. F., Steinmetz, M., & Eke, V. R. 2003, ApJ, 597, 21
Barmby, P. 2003, in Extragalactic Globular Cluster Systems, ed. M. Kissler-Patig (Berlin: Springer), 143
Barmby, P., Holland, S., & Huchra, J. P. 2002, AJ, 123, 1937
Barmby, P., & Huchra, J. P. 2001, AJ, 122, 2458
Barmby, P., Huchra, J. P., Brodie, J. P., Forbes, D. A., Schroder, L. L., & Grillmair, C. J. 2000, AJ, 119, 727
Battistini, P. L., Bonoli, F., Braccesi, A., Federici, L., Fusi Pecci, F., Marano, B., & Borngren F. 1987, A&AS, 67, 447
Battistini, P. L., Bonoli, F., Braccesi, A., Fusi Pecci, F., Malagnini, M. L., & Marano, B. 1980, A&AS, 42, 357
Battistini, P. L., Bonoli, F., Buonanno, R., Corsi, C. E., & Fusi Pecci, F. 1982, A&A, 113, 39
Beasley, M. A., Brodie, J. P., Strader, J., Forbes, D. A., Proctor, R. N., Barmby, P., & Huchra, J. P. 2004, AJ, 128, 1623
Bertone, E. 2001, Ph.D. thesis, Milan Univ.
Bertone, E., Rodriguez-Merino, L. H., Chavez, M., & Buzzoni, A. 2003, Rev. Mex. AA Ser. Conf., 17, 91
Bohlin, R. C., Cornett, R. H., Hill, J. K., Hill, R. S., & Stecher, T. P. 1988, ApJ, 334, 657
Bohlin, R. C., et al. 1993, ApJ, 417, 127
Brodie, J. P., & Hanes, D. A. 1986, ApJ, 300, 258
Brodie, J. P., & Huchra, J. P. 1990, ApJ, 362, 503
Brown, T. M., Ferguson, H. C., Smith, E., Kimble, R. A., Sweigart, A. V., Renzini, A., Rich, R. M., & VandenBerg, D. A. 2003, ApJ, 592, L17
Bruzual, G., & Charlot, S. 2003, MNRAS, 344, 1000
Buonanno, R., Corsi, C. E., Battistini, P., Bonoli, F., & Fusi Pecci, F. 1982, A&AS, 47, 451
Burstein, D., Faber, S. M., Gaskell, C. M., & Krumm, N. 1984, ApJ, 287, 586
Burstein, D., et al. 2004, ApJ, 614, 158
Buzzoni, A. 1989, ApJS, 71, 817
———. 1995a, ApJS, 98, 69
———. 1995b, in ASP Conf. Ser. 86, Fresh Views of Elliptical Galaxies, ed. A. Buzzoni, A. Renzini, & A. Serrano (San Francisco: ASP), 189
———. 2002, AJ, 123, 1188
Buzzoni, A., Mantegazza, L., & Gariboldi, G. 1994, AJ, 107, 513
Chandar, R., Bianchi, L., & Ford, H. C. 1999, ApJS, 122, 431
Cowley, A. P., & Burstein, D. 1988, AJ, 95, 1071
Crampton, D., Cowley, A. P., Shade, D., & Chayer, P. 1985, ApJ, 288, 494
Cutri, R. M., et al. 2003, Explanatory Supplement to the 2MASS All Sky Data Release, http://www.ipac.caltech.edu/2mass/releases/allsky/doc/explsup.html
Elson, R. A. W., & Fall, S. M. 1985, PASP, 97, 692
Elson, R. A. W., & Walterbos, R. A. M. 1988, ApJ, 333, 594
Faber, S. M., Friel, E. D., Burstein, D., & Gaskell, C. M. 1985, ApJS, 57, 711
Freedman, W. L., & Madore, B. F. 1990, ApJ, 365, 186
Galleti, S., Federici, L., Bellazzini, M., Fusi Pecci, F., & Macrina, S. 2004, A&A, 416, 917
Gorgas, J., Faber, S. M., Burstein, D., González, J. J., Courteau, S., & Prosser, C. 1993, ApJS, 86, 153
Harris, W. E. 1996, AJ, 112, 1487
———. 2001, in Star Clusters, ed. L. Labhardt & B. Biggeli (Berlin: Springer), 223

Hodge, P. W. 1979, AJ, 84, 744
———. 1992, The Andromeda Galaxy (Dordrecht: Kluwer)
Ibata, R., Chapman, S., Ferguson, A. M. N., Irwin, M., Lewis, G., & McConnachie, A. 2004, MNRAS, 351, 117
Jiang, L., Ma, J., Zhou, X., Chen, J., Wu, H., & Jiang, Z. 2003, AJ, 125, 727
Johnson, H. L. 1966, ARA&A, 4, 193
King, J. R., & Lupton, R. H. 1991, in ASP Conf. Ser. 13, The Formation and Evolution of Star Clusters, ed. K. Janes (San Francisco: ASP), 575
Kurth, O. M., Fritze-v. Alvensleben, U., & Fricke, K. J. 1999, A&AS, 138, 19
Lee, H.-C., Yoon, S.-J., & Lee, Y.-W. 2000, AJ, 120, 998
McClure, R. D., & Racine, R. 1969, AJ, 74, 1000
Mermilliod, J.-C. 1995, in ASP Conf. Ser. 90, The Origins, Evolution, and Destinies of Binary Stars in Clusters, ed. E. F. Milone & J.-C. Mermilliod (San Francisco: ASP), 475
Morrison, H., Harding, P., Perrett, K. M., & Hurley-Keller, D. 2004, ApJ, 603, 87
Perrett, K. M., Bridges, T. J., Hanes, D. A., Irwin, M. J., Brodie, J. P., Carter, D., Huchra, J. P., & Watson, F. G. 2002, AJ, 123, 2490
Peterson, R. C., Carney, B. W., Dorman, B., Green, E. M., Landsman, W., Liebert, J., O'Connell, R. W., & Rood, R. T. 2003, ApJ, 588, 299
Puzia, T. H., Perrett, K. M., & Bridges, T. J. 2005, A&A, 434, 909
Puzia, T. H., Saglia, R. P., Kissler-Patig, M., Maraston, C., Greggio, L., Renzini, A., & Ortolani, S. 2002, A&A, 395, 45
Renzini, A., & Buzzoni, A. 1986, in Spectral Evolution of Galaxies, ed. C. Chiosi & A. Renzini (Dordrecht: Reidel), 195
Rich, R. M. 2003, in ASP Conf. Ser. 296, New Horizons in Globular Cluster Astronomy, ed. G. Piotto et al. (San Francisco: ASP), 533
Sargent, W. L. W., Kowal, C. T., Hartwick, F. D. A., & van den Bergh, S. 1977, AJ, 82, 947
Scheffler, H. 1982, in Landolt-Börnstein Zahlenwerte und Funktionen aus Naturwissenschaften und Technik: Neue Serie, Group 6, Vol. 2, ed. L. H. Aller et al. (Berlin: Springer), 46
Schiavon, R. P., Rose, J. A., Courteau, S., & MacArthur, L. 2004, ApJ, 608, L33
Searle, L. 1978, NATO Advanced Study Institute on Globular Clusters (Cambridge: Cambridge Univ. Press)
Sharov, A. F., Lyutyi, V. M., & Esipov, V. F. 1995, Astron. Lett., 21, 240
Spinrad, H., & Schweizer, F. 1972, ApJ, 171, 403
Tinsley, B. M., & Gunn, J. E. 1976, ApJ, 203, 52
Tripicco, M. J. 1989, AJ, 97, 735
van den Bergh, S. 1967, AJ, 72, 70
———. 1969, ApJS, 19, 145
———. 1981, A&AS, 46, 79
———. 1991, ApJ, 369, 1
———. 2000, The Galaxies of the Local Group (Cambridge: Cambridge Univ. Press)
Veteŝnik, M. 1962, Bull. Astron. Inst. Czechoslovakia, 13, 180
Williams, B. F., & Hodge, P. W. 2001a, ApJ, 548, 190
———. 2001b, ApJ, 559, 851
Worthey, G. 1994, ApJS, 95, 107